Studying Short-Range Correlations in Nuclei at the Repulsive Core Limit via the Triple Coincidence $(e, e'pN)$ Reaction

R. Guy, *E. Piasetzky (spokesperson)*[1], J. Lichtenstadt I. Pomerantz, and R. Shneor

Tel Aviv University, Tel Aviv, Israel

W. Bertozzi, *S. Gilad (spokesperson)*, J. Huang, *B. Moffit (spokesperson)*, P. Monaghan, N. Muangma, A. Puckett, Y. Qiang, and X. Zhan,

Massachusetts Institute of Technology, Cambridge, MA, USA

B.D. Anderson, A.R. Baldwin, G. Petratos, *J.W. Watson (spokesperson)*, R. Subedi, and W-Ming Zhang

Kent State University, Kent, OH, USA

E. Chudakov, J.P. Chen, J.-O. Hansen, *D.W. Higinbotham (spokesperson)*, M. Jones, J.-M. Laget, J.J. LeRose, D. Meekins, A. Saha, and S. Wood

Thomas Jefferson National Accelerator Facility, Newport News, VA, USA

V. Sulkosky

College of William and Mary, Williamsburg, VA, USA

W. Boeglin and P. Markowitz

Florida International University, Miami, FL, USA

A. Beck and S. Maytal-Beck

Nuclear Research Center Negev, Beer-Sheva, Israel

L. Weinstein

Old Dominion University, Norfolk, VA, USA

Seonho Choi, Ho-young Kang, Hyekoo Kang, Byungwuek Lee, Yoomin Oh, and Jeongseog Song

Seoul National University, Seoul, Korea

Jefferson Lab PAC31 Proposal *11 December 2006*

B. Sawatzky

Temple University, Philadelphia, PA, USA

R.J. Peterson

University of Colorado, Boulder, CO, USA

J. Annand, D. Ireland, D. Protopopescu, and G. Rosner

University of Glasgow, Glasgow, Scotland, UK

M. Potokar and S. Širca

University of Ljubljana, Slovenia

F. Benmokhtar

University of Maryland, College Park, MD, USA

D. Day, R. Lindgren, N. Liyanage, B. Norum, and K. Wang

University of Virginia, Charlottesville, VA, USA

A. Shahinyan

Yerevan Physics Institute, Yerevan, Armenia

Abstract

One of the original motivations for building Jefferson Lab was to understand short-range nucleon-nucleon (NN) correlations. Our first high luminosity triple coincidence experiment, E01-015, measured the $(e, e'pp)$ and $(e, e'pn)$ reactions over the $(e, e'p)$ missing momentum range from 300 to 500 MeV/c and was sensitive to the short-range NN tensor force. We now propose to measure these reactions on ^{4}He over the missing momentum range from 400 to 875 MeV/c in order to study the NN short-range repulsive force. The proposed kinematic conditions (large Q^2 and $x_B > 1$) allow us to extract the abundance of np and pp correlated pairs with minimal obstacles from final state interactions, meson exchange currents, and resonance production.

The experiment will use the standard Hall A cryotarget and the two standard high resolution spectrometers to measure the ^{4}He$(e, e'p)$ part of the reaction. The BigBite spectrometer and an array of scintillation counters will detect the recoiling protons and neutrons; allowing us to measure the $(e, e'pp)$ and $(e, e'pn)$ reactions simultaneously.

We are requesting 29 days of beam time to perform these measurements.

[1] contact person: Eli Piasetzky, eip@tauphy.tau.ac.il

1 Introduction

1.1 Scientific background

> "The structure of correlated many-body systems, particularly at distance scales small compared to the radius of the constituent nucleons, presents a formidable challenge to both experiment and theory" - Nuclear Science: A Long Range Plan, February 1996 [1].

The interplay between the attractive and the repulsive short-range components of the nucleon-nucleon force causes some of the nucleons inside a nucleus to form pairs that have a low center-of-mass momentum and a high relative momentum [2–4] (relative to the Fermi sea level, k_F). We refer to such pairs herein as two-nucleon short-range correlations (2N-SRC).

In the last decade, utilizing high energy electron-nucleus scattering measurements at JLab, we have identified 2N-SRC, studied their structure, and related them to the underlying basic short-range nucleon-nucleon (NN) interaction.

At short distances the dominating NN forces involved are the tensor force and the short-range repulsive force. Experiment E01-015 [5,6] measured 2N-SRC associated with electrons interacting with protons above the Fermi sea level with momentum of 300-600 MeV/c. The results of that experiment, as presented in this proposal, indicate that in this range the dominant contribution is from the tensor force. **This proposal will extend the study to larger momenta in order to explore the elusive repulsive core of the NN interactions.**

For $Q^2 > 1$ $(\mathrm{GeV/c})^2$, measurements in Hall B [7,8] observed x_B scaling in the ratios of inclusive (e, e') cross sections on heavy nuclei to the cross sections on ^{3}He when x_B is larger than 1.4. These measurements confirmed the earlier observation of scaling for nucleus-to-deuteron cross section ratios [9], indicating that the electron probes high momentum nucleons coming from local sources in the nuclei (i.e SRC). These sources are sensitive to the short-range forces between two close nucleons but in general are independent of the non-correlated residual nucleus. The overall probability for a nucleon in ^{12}C to be a member of a two-nucleon SRC state, proton-proton (pp), neutron-proton (np), or neutron-neutron (nn), was estimated from the x_B-dependence of inclusive (e, e') data to be $(20 \pm 5)\%$ [7,8]. The same work [8] shows that the probability of 3N-SRC is about an order of magnitude lower that the probability of finding a SRC pair in the nucleus. **The inclusive (e, e') measurements do not supply any information on the isospin structure of the 2N-SRC.**

The indications that inclusive electron scattering at large x_B probe high momentum bound nucleons from 2N-SRC has been confirmed by high energy, large momentum transfer $^{12}\mathrm{C}(p, pp)$ and $^{12}\mathrm{C}(p, ppn)$ measurements [10–13] done at EVA/BNL (Figure 1). This triple coincidence measurement directly observed the existence of correlated np pairs with a yield consistent with the (e, e') results [14].

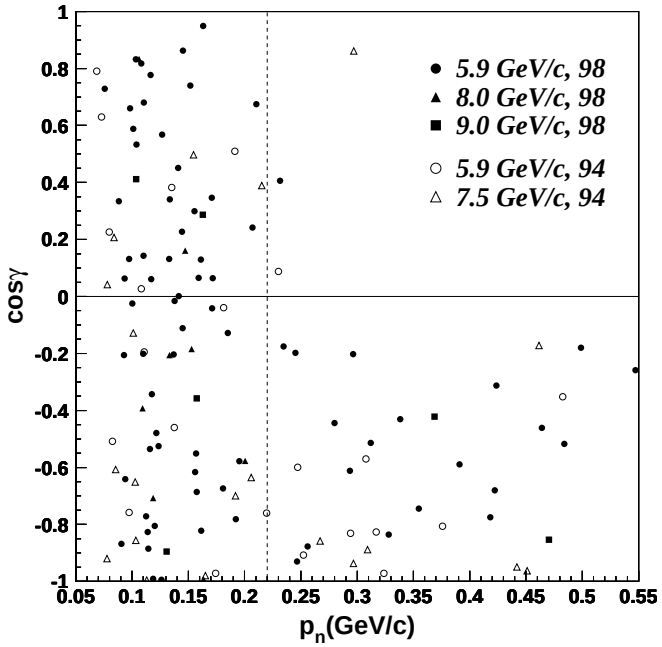

Fig. 1. The correlation between the neutron momentum p_n and its direction γ relative to the momentum of the struck proton. Data labeled by 94 and 98 are from Ref. [10] and [11] respectively. The momenta are the beam momenta. The dotted vertical line corresponds to $k_F = 220$ MeV/c [15].

Recent analysis [13] of these data shows that the high momentum tail in nuclei is dominated by 2N-SRC and that the 2N-SRC are dominated by np-SRC pairs. In ^{12}C, $74-100\%$ of the protons with momentum above 275 MeV/c are members of an np-SRC pair. **The EVA/BNL results indicate a large abundance of np-SRC over pp-SRC. The errors on this determination are large so that the EVA/BNL data alone can only allow to set an upper limit of about 17% on the pp-SRC/np-SRC ratio in ^{12}C.**

The pp-SRC pairs were observed in a subsequent measurement at JLab (E01-015) [5,6]. A simultaneous measurement of the triple coincidence $^{12}\mathrm{C}(e,e'pp)$ and double coincidence $^{12}\mathrm{C}(e,e'p)$ reactions reveal that the ratio of $(e,e'pp)$ to $(e,e'p)$ events for $(e,e'p)$ missing momentum above 300 MeV/c is $(7\pm2)\%$ (shown in Figure 2). Combining this with the EVA/BNL data, leads to the estimate of $92^{+5}_{-18}\%$ of np-SRC pairs and $(3.5\pm1)\%$ pp-SRC pairs for protons above 300 MeV/c in ^{12}C.

If one combines the determination of the np-SRC amount from the EVA/BNL measurement with the amount of the pp-SRC, from the E01-015 data, one obtains a much better upper limit to the pp-SRC/np-SRC ratio:

$$\frac{pp-\mathrm{SRC}}{np-\mathrm{SRC}} = \frac{3.5\pm1\%}{74-95\%} \leq 6\% \qquad (1)$$

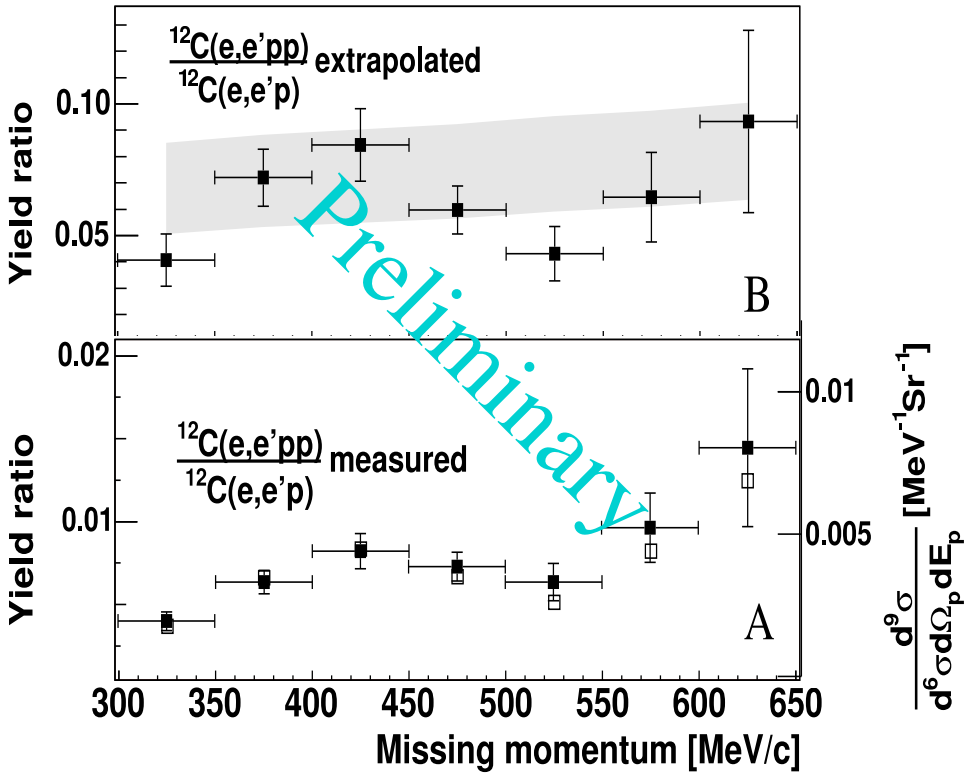

Fig. 2. The measured (**A**) and extrapolated (**B**) ratios of yields for the ^{12}C$(e,e'pp)$ and the ^{12}C$(e,e'p)$ reactions. The full squares in **A** are the yield ratios and the open squares are the corresponding ratios of the differential cross sections for the ^{12}C$(e,e'pp)$ reaction to the ^{12}C$(e,e'p)$ reaction. The gray area in **B** represents a band of $\pm 5\sigma$, uncertainty in the width of the CM momentum of the pair. This value and its associated uncertainty were extracted from the data.

Data from experiment E01-015 allows a direct determination of the ratio of *pp*-SRC to *np*-SRC pairs from the measured ratio of ^{12}C$(e,e'pp)/^{12}$C$(e,e'pn)$ reactions. Preliminary results, to be presented to this PAC, are consistent with the value shown above in Eq.(1).

The small ratio of *pp*/*np* as observed by the EVA/BNL and E01-015 experiments stimulated work by two theoretical groups [16,17]. Both theoretical groups show that the measured *pp*-SRC/*np*-SRC ratio is expected and is a clear indication of the NN tensor force at the probed distances and relative momentum of the nucleons in the SRC pair. R. Schiavilla and M. Strikman presented preliminary results at the SRC2006 Workshop [18]. The Argonne group already submitted a letter [17,19] on this work. These theoretical conclusions are in agreement with earlier studies of $n(k)$ for large momenta that also indicated dominance of tensor correlations [20,21].

R. Schiavilla et al. [17,19] calculated the 2N momentum distributions for the ground states of light nuclei ($A \leq 8$) using variational Monte Carlo wave functions derived from a realistic Hamiltonian with two- and three-nucleon potentials (shown in Figure 3). Their

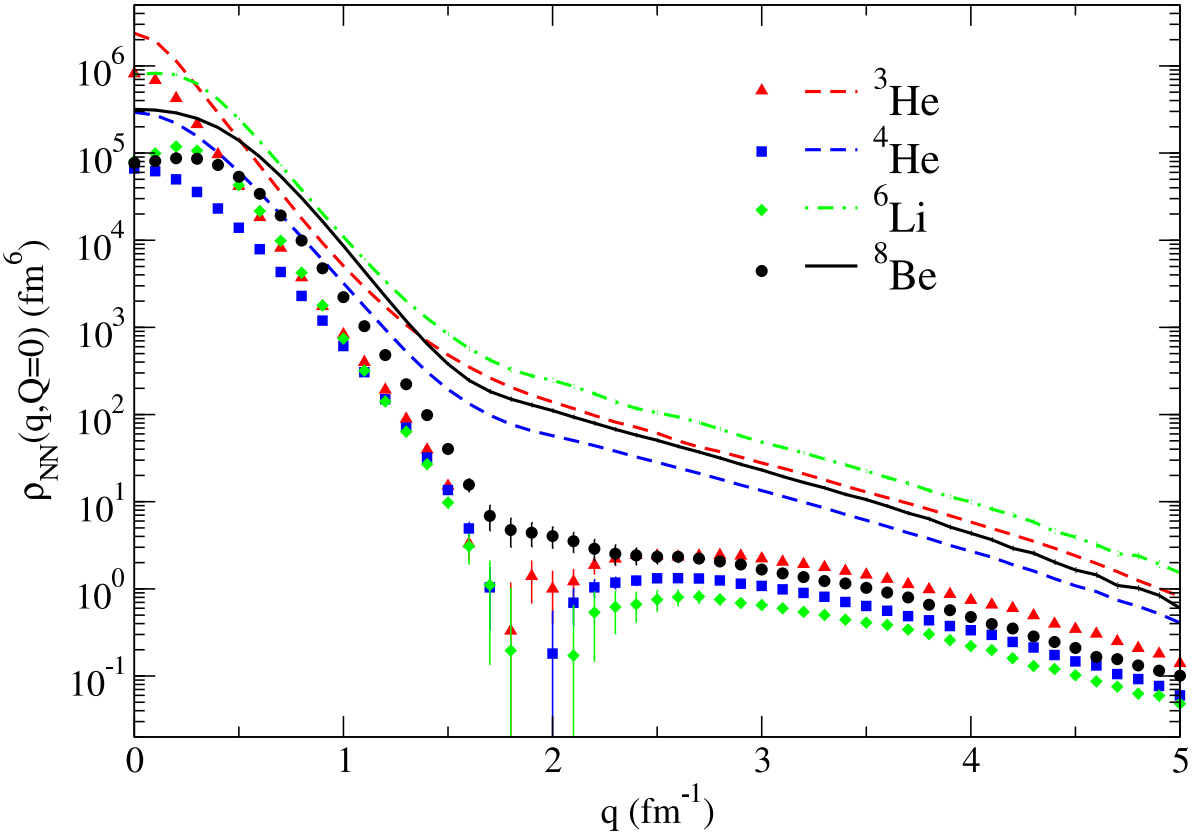

Fig. 3. The momentum distribution for np (lines) and pp (symbols) pairs in various nuclei [19]. The calculations assume pairs at rest ($Q = 0$) as a function of the relative momentum of the nucleons in the pair (q).

calculation for CM motion at rest ($Q = 0$) show a large np/pp ratio at the relative momentum range, $q = 300 - 600$ MeV/c, which has a universal character originating from the tensor component of the NN force. They also predict the ratio for larger q values.

M. Sargsian et al. [16,22], in the framework of generalized Eikonal approximation, calculated for ^{3}He the decay function and differential cross section for the $(e, e'pp)$ and $(e, e'pn)$ reactions taking into account the ground state properties as well as FSI (see definition of the decay function in Section 2.1.1). This calculation uses realistic wave functions with two- and three-nucleon forces. In Figure 4, we show the density distribution for np and pp pairs in ^{3}He. This calculation represents integration over a CM momentum of the pair in the range of $0 - 150$ MeV/c. For the purpose of this proposal we corrected the calculated pp/np ratio for ^{3}He by a combinatorial factor that takes into account the difference in the ratio of pp to np pairs in the two nuclei. We neglect any difference resulting from the different ground state wave functions.

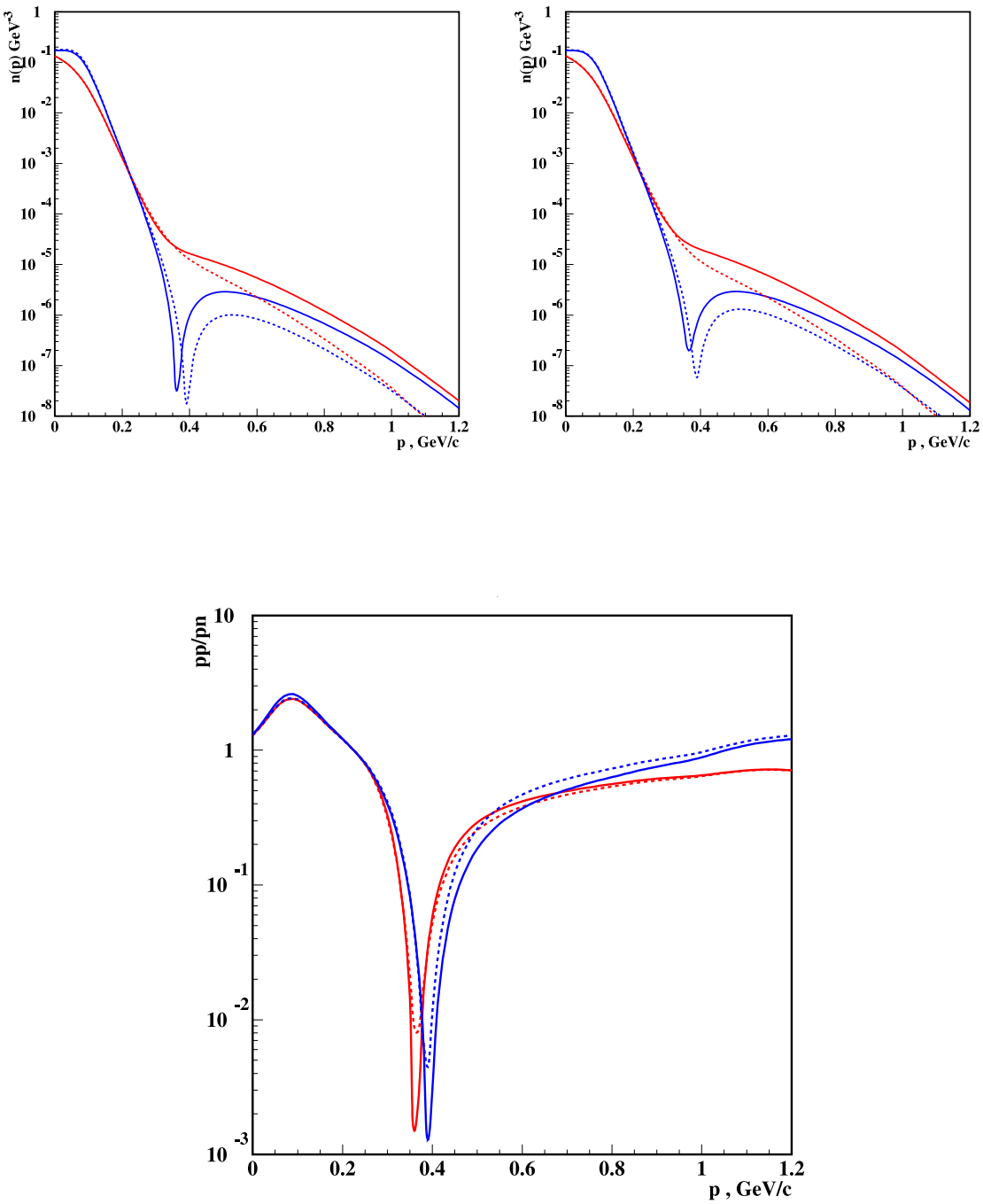

Fig. 4. The density distribution for *np* (red) and *pp* (blue) pairs in ^{3}He [16,22]. The calculations assume that the pairs have CM momentum up to 150 MeV/c and use the Argonne V18 potential (solid) or the Bonne potential (dashed). The three nucleon forces are included in the left figure but not in the right one. The lower figure shows the *pp*/*np* ratio with/without three nucleon forces (dashed/solid lines) included for V18 (red) and Bonne (blue) potentials.

Just to clarify, Figure 5 presents an estimate of the $(e,e'pp)/(e,e'pn)$ ratio for ^{4}He based on the of pp/np density calculations by the Argonne group [17,19] and M. Sargsian for ^{3}He [22] (scaled to take into account the ratio of pp to np pairs in ^{4}He). Overlaid are the data for ^{12}C deduced from the BNL and E01-015 experiments (scaled to take into account the pair counting in ^{12}C compared to ^{4}He). The proposed new measurements are also shown, arbitrarily set between the V18 and the Bonne potential calculations of Ref. [22]. All quantities shown here are functions of $q = p_{\rm miss}$. The measurement uncertainty of the proposed points are dominated by the statistics of the $(e,e'pn)$ measurement (assumed to be 25%).

1.2 The motivation for the current proposal

The association of the small ^{12}C$(e,e'pp)/^{12}$C$(e,e'pn)$ ratio ($\leq$6 %) with the dominance of the NN-SRC tensor force leads naturally to the quest to increase the missing momentum and to look for pairs which are even closer to each other, at such distances that are dominated by the repulsive core. The repulsive core, which is essentially unexplored experimentally, is considered to be a scaler force.

If we look at the calculated ratio for pairs in ^{3}He, we can see that above about 850 MeV/c the ratio of pp/np in ^{3}He is about 0.5-0.7. This is about an order of magnitude higher than what was measured for ^{12}C at $p_{\rm miss}$ below 500 MeV/c [5,6,23]. The expected rise of the ratio is theoretically associated with the onset of the repulsive force dominance. The increase in the ratio can be due to a reduction in the number of np-SRC, an increase in the number of pp-SRC, or both decreasing but with a very different slope (the np-SRC decreasing much faster than the pp-SRC as a function of the missing momentum).

We propose to simultaneously measure the ^{4}He$(e,e'pp)/^4$He$(e,e'p)$, ^{4}He$(e,e'pn)/^4$He$(e,e'p)$, and ^{4}He$(e,e'pp)/^4$He$(e,e'pn)$ ratios for missing momenta in the 400-875 MeV/c range and to learn about the elusive NN repulsive core. Since there are already two theoretical groups interested in the results and since the repulsive core in the NN interaction is such an important fundamental subject, we are certain that the new data, perhaps even this proposal, will trigger theoretical works that will relate the observables to the underlying short-range NN physics.

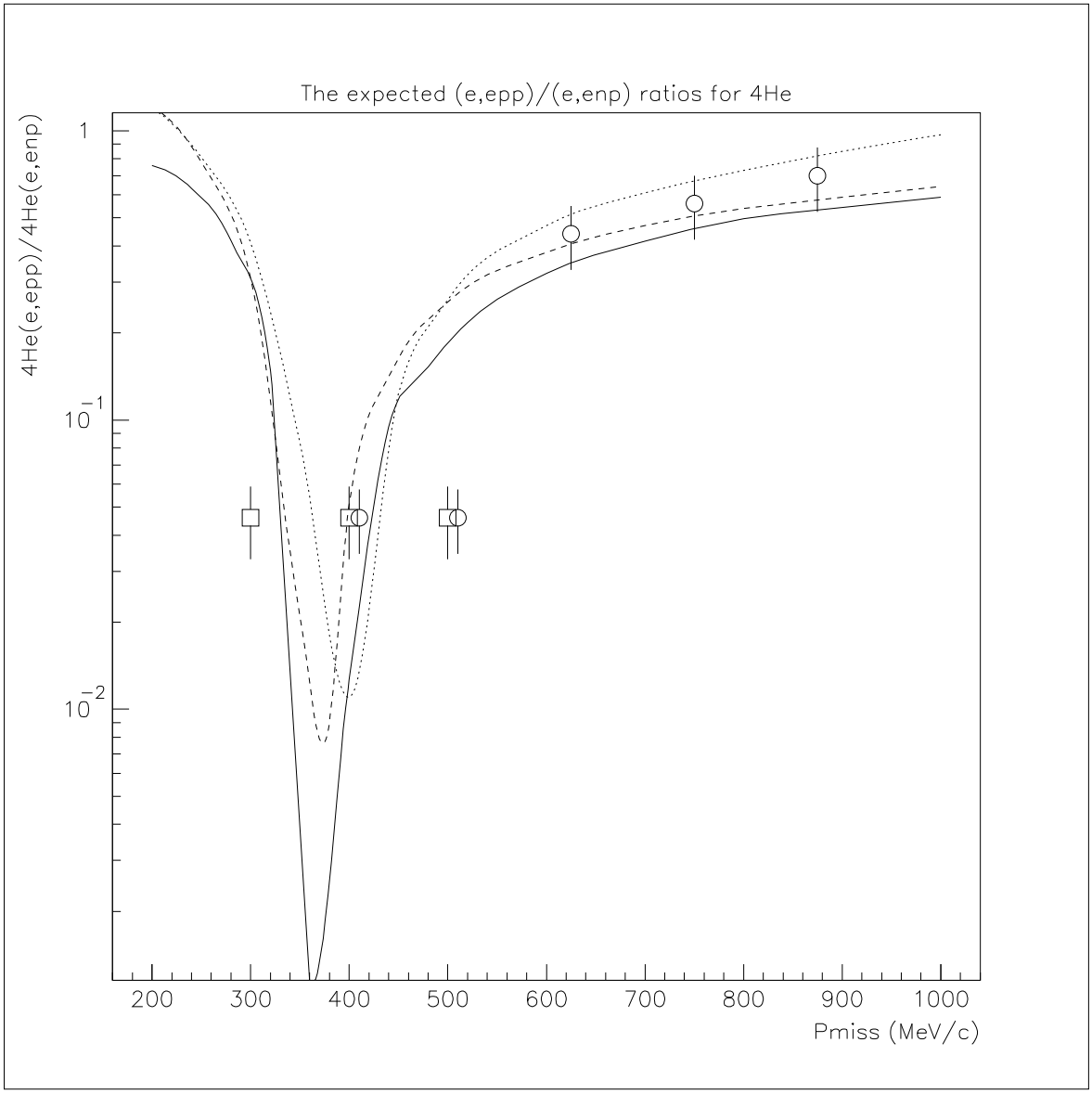

Fig. 5. The predicted ^{4}He$(e,e'pp)$/ ^{4}He$(e,e'pn)$ ratio as a function of $p_{\rm miss}$. The preliminary measured ratio for ^{12}C (open squares) scaled to ^{4}He and the proposed measurements (open circles) are also shown. These points were set arbitrarily between the V18 and the Bonne potential calculations of Ref. [22].

2 The Proposed Measurement

2.1 The selected kinematics for the measurement

The kinematics chosen for E01-015 and for the current proposal are optimized to allow identification of the 2N-SRC pairs and to suppress contributions from competing effects.

2.1.1 Kinematical characteristics of NN SRC at rest

The signature of the short range nature of a NN interaction is the strong correlation between *the momenta* of the correlated nucleons. Thus, for a pair at rest, when knocking out one of the nucleons, the second (spectator) nucleon will have a momentum (p_s) which is balanced with the missing momentum of the knocked out nucleon: ($\vec{p}_s \approx -\vec{p}_m$). Since SRC will exist predominantly in the high momentum tail of the nuclear wave function, such a spectator should have a large p_s, $p_s \geq k_F \approx 250\ MeV/c$.

We discuss the quasi-free break-up reaction of the pair at rest and we denote the pair, at rest in the nucleus, as d (deuteron):

$$e + d \rightarrow e' + p + n. \tag{2}$$

The kinematical conditions of the quasi-elastic reaction sets:

$$(q + p_d - p_f)^2 = m^2, \tag{3}$$

where $q = (q_0, \vec{q})$, $p_d = (m_d, \vec{0})$ and $p_f = (E_f, \vec{p}_f)$ are the four-momenta of the virtual photon, the target pair and the detected final nucleon, respectively. From the $(e, e'p)$ information we determine the missing momentum as $\vec{p}_m = \vec{p}_f - \vec{q}$ and the missing energy as $E_m = q_0 - (E_f - m)$. From Eq.(3) we obtain the following relation between missing momentum and energy:

$$E_m = \sqrt{m^2 + p_m^2} + m - m_d \approx \frac{p_m^2}{2m}. \tag{4}$$

Thus, in the breakup of a pair, there is a strong correlation between the measured missing momentum p_m and the missing energy E_m.

The decay function is the joint probability to remove a nucleon from the nucleus with missing energy/momentum E_m/p_m and to have a recoil nucleon in the residual A-1 nucleus with $\vec{p}_s$. In terms of the decay function we concentrate on:

$$D(E_m = p_m^2/2m, p_m > k_F, \vec{p}_s = -\vec{p}_m). \tag{5}$$

2.1.2 Suppression of competing effects.

Historically, the interpretation of electron scattering data in terms of SRC has been plagued by contributions from the large single particle (mean field) contribution as well as meson exchange currents (MEC), isobar currents (IC) and final-state interactions (FSI). The kinematics for the measurement described herein were chosen to allow the study of the small spatial size of SRCs and minimize these competing effects.

The kinematics we chose for E01-015 and for the current proposal are at a high beam energy, a large Q^2, $x_B > 1$, a large $(e, e'p)$ missing momentum and large matching missing energy. These conditions, together with the exclusiveness of the triple coincidence measurement, allow us to identify clearly the 2N-SRC and measure their abundance [5,6,23].

A large Q^2 is required if one wishes to study the structure of an object of the size of the 2N-SRC. A high Q^2 value also reduces the MEC contributions, which decreases as $1/Q^2$, relative to the SRC contribution [24,25]. A large Q^2 is also required to probe high missing-momentum values in the $(e, e'p)$ reaction with $x_B > 1$, which reduces drastically the isobar production contribution. Finally, we minimize FSI by having a large $\vec{p}_{\rm miss}$ component anti-parallel to the virtual photon direction [26].

The FSI in the $(e, e'pp)$ and $(e, e'pn)$ reactions occur between the nucleons in the SRC pair, as well as interactions of these pairs with the other nucleons in the residual A-2 system. The interaction between nucleons in the pair conserves the isospin structure of the pair (i.e. pp/np pairs remain as pp/np pairs). The FSI between members of the SRC pair also do not change the CM momentum of the pair as reconstructed from the momentum of the detected particles.

The FSI of the recoiling protons with the rest of the nucleus is strongly suppressed due to Pauli blocking [27]. Moreover, according to Ref. [26], the large anti-parallel component of $\vec{p}_{\rm miss}$ ensures the scattering was on an SRC pair and reduces the FSI contribution. The elastic (real) part of the FSI can alter the momenta, such that to make $\vec{p}_{\rm miss} \neq \vec{p}_1$, $\vec{p}_{rec} \neq \vec{p}_2$ and $\vec{p}_{\rm CM}$ different from

$$\vec{p}_{\rm CM} = \vec{p}_{\rm rec} + \vec{p}_{\rm HRS-R} - \vec{q}. \tag{6}$$

The absorptive (imaginary) part can reduce the $^{12}{\rm C}(e, e'pp)/^{12}{\rm C}(e, e'p)$ ratio, while single charge exchange can turn np-SRC pairs into $^{12}{\rm C}(e, e'pp)$ events, thereby increasing the measured ratio. These two latter effects almost balance each other. Our simple estimates of the FSI effects, based on a Glauber approximation using the method described in Ref. [28], indicate that the contribution of FSI with the A-2 system are small compared to the expected statistical uncertainties in the measurement.

This conclusion is supported by the E01-015 data [23]. The CM momentum of the pair, extracted as described above, is a combination of the CM motion and the effect of FSI. The fact that we get widths of both longitudinal and transverse components of CM momentum

distributions that are narrow and consistent with a previous measurement, indicates that the FSI contribution to this observable cannot be dominant. We will be able to test this prediction by comparing the ^{4}He and ^{12}C measurements.

The small result of the measured ratio of $^{12}\mathrm{C}(e,e'pp)/^{12}\mathrm{C}(e,e'pn)$, which is a result of the tensor nature of the NN interaction, is another indication that FSI do not smear the basic NN SRC physics. One would expect the node in the *pp* momentum distribution to be filled in by the FSI. However, as the E01-015 data indicate, the measured cross-section ratio still reflect the genuine ground state momentum distribution. To extract from the data the exact ground state properties, one needs realistic treatment of the SRC and the FSI. The proposed study on light nuclei (^{4}He) will make these calculations more accessible. We expect that even without the exact calculation the measured ratio will reflect the underlying physics of the transition from the tensor force minimum in the ratio to larger ratios induced by the repulsive core part of the short-range interaction.

2.1.3 The Detailed Kinematics for the Measurements

We propose to measure the triple coincidence of a small cross section (pb/MeVsr^2) corresponding to an elusive feature in nuclear physics. We have chosen a large incident energy ($\sim$ 5 GeV), large Q^2, large target proton momentum, and large x_B to minimize competing nuclear effects.

The proposed measurement is reasonably flexible with the incident electron energy (between 4.5 and 5.1 GeV). Table 1 summarizes the proposed kinematics, assuming an incident electron energy of 4.8 GeV. The Left HRS is fixed to detect 3.95 GeV scattered electrons at 18.7° to obtain $Q^2 = 2.0$ (GeV/c)^2. The Right HRS momentum and angle is scanned to cover a range of missing momentum p_{miss} in the $(e,e'p)$ reaction of 400 MeV/c to 875 MeV/c. For all of the kinematics listed $|\vec{q}| = 1.131$ GeV/c, $\theta_q = 50.1°$, and $x_B = 1.25$. To detect the recoiling nucleon, the BigBite spectrometer and neutron detector will be placed at about 96° for K1 through K3, and about 89° for K4 and K5.

Kinematic	p_{miss} [GeV/c]	Proton Momentum [GeV/c]	Proton Angle degree	Recoil Angle degree
K1	0.405	1.415	37.7°	98.6°
K2	0.491	1.370	34.7°	98.0°
K3	0.627	1.285	30.0°	95.0°
K4	0.755	1.190	25.5°	91.2°
K5	0.873	1.090	21.2°	87.2°

Table 1
Proposed kinematics showing the range of missing momentum p_{miss} obtained by selecting the momentum and angle of the quasi-elastic breakup proton with the Right HRS. With an incident beam energy of 4.8 GeV and the Left HRS detecting 3.95 GeV scattered electrons at 18.7°, the BigBite spectrometer and the neutron array will be positioned at about 96° for K1 through K3 and about 89° for K4 and K5.

3 Experimental Setup

The experimental setup for the proposed measurement, parallels that which was used for Experiment E01-015. In this section, we review the E01-015 setup and then state the proposed changes required for the new measurements. We conclude with an estimation of the triple coincidence rates for each kinematic and a summary of our requested beam time.

3.1 Experiment E01-015 setup

Experiment E01-015 was performed in Hall A of the Thomas Jefferson National Accelerator Facility (JLab) using an incident electron beam of 4.627 GeV with a current between 5 and 30 μA. The target was a 0.25 mm graphite foil tilted 20° with respect to the beam line to minimize the material through which the low-energy recoiling proton passed. The Hall A two high-resolution spectrometers (HRS) [29] were used to measure the ^{12}C$(e, e'p)$ reaction.

The scattered electrons were detected in the left HRS (HRS-L) at a central scattering angle (momentum) of 19.5° (3.723 GeV/c). This corresponds to the quasi-free knockout of a single proton with transferred three-momentum $|\vec{q}| = 1.67$ GeV/c, transferred energy $\omega = 0.904$ GeV, $Q^2 = 2$ (GeV/c)^2, and $x_B = \frac{Q^2}{2M\omega} = 1.2$.

The knocked-out protons were detected using the right HRS (HRS-R) which was set at 3 different combinations of central angle and momentum: 40.1° & 1.45 GeV/c, 35.8° & 1.42 GeV/c and 32.0° & 1.36 GeV/c. These kinematic settings correspond to missing-momentum values $p_{\rm miss} = 0.31$, 0.41 and 0.52 GeV/c, respectively. Figure 6 shows a schematic of the layout for the highest $p_{\rm miss}$ kinematic. The combined acceptance of the two HRSs restricted the missing-momentum range in each setting to about ± 0.050 GeV/c.

BigBite was used to detect the recoiling proton in the ^{12}C$(e, e'pp)$ events. The BigBite spectrometer [30] (shown in Figure 7) consists of a large-acceptance, non-focusing dipole magnet located at an angle of 99° and 1.1 m from the target with a resulting angular acceptance of about 96 msr and a nearly unlimited momentum acceptance starting from 0.25 GeV/c. A custom, unshielded BigBite detection package was constructed for this experiment. It consisted of three planes of plastic scintillator segmented in the dispersive direction. The first scintillator plane (the auxiliary plane) was placed at the exit of the dipole, parallel to the magnetic field boundary and was made-up of 56 narrow scintillator bars of dimension 250x25x2.5 mm^3. The second (ΔE) and third (E) scintillator planes were mounted together and were located 1 meter downstream of the first plane. The second and third layers consisted of 24 scintillator bars each, with dimensions 500x86x3 mm^3 and 500x86x30 mm^3 respectively. The scintillator bars in these two layers were offset from one another by half a bar in the dispersive plane, improving their position resolution by a factor of two to 43 mm. Each of the scintillator bars in the auxiliary plane was read out

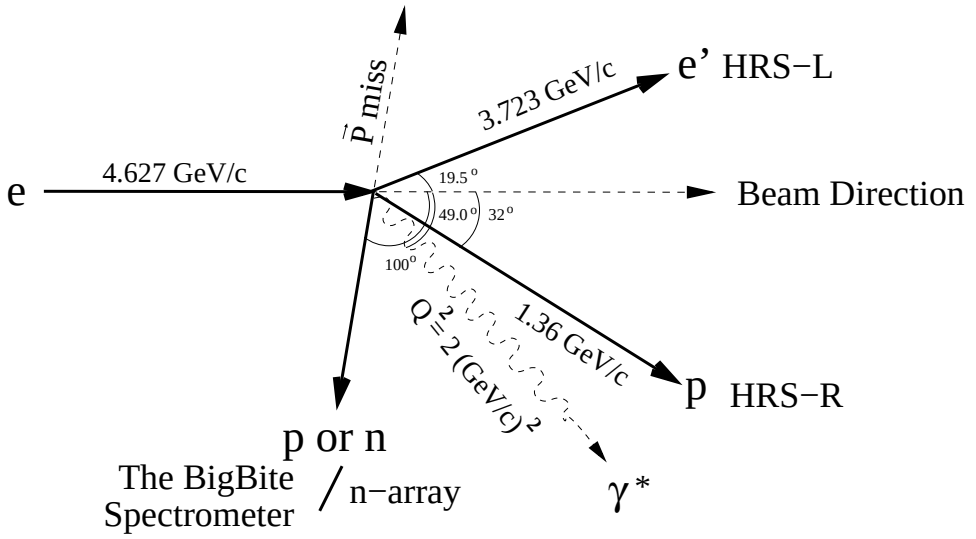

Fig. 6. The layout of E01-015 for the largest $P_{\rm miss}$ kinematics of 0.5 GeV/c.

by one photomultiplier tube (PMT), while each of the ΔE and E scintillator was read out by two PMTs on both ends of each bar. This unshielded system was able to run in Hall A up to a luminosity of 10^{38} cm^{-2}s^{-1}.

The recoil neutrons were detected using 88 plastic scintillator bars covering an area of 1x3 m^2 and 0.4 m deep. Each bar was 10 cm thick in the beam direction and 1 m long. The bars were arranged in four planes, with height varying from 10 cm for the first plane to 25 cm for the fourth plane. In front of the first layer of bars there was a 5 cm lead wall designed to block low-energy photons and most of the charge particles. This was followed by a layer made up of 2 cm thick 64 plastic counters that served to identify charge particles that passed the lead wall. The neutron detector array was placed six meters from the target, just behind BigBite, covering a similar solid angle as BigBite.

A model of the neutron detection efficiency, incorporating the transmittance of neutrons through material between the target and detector [31] and the efficiency of the scintillator planes [32], is shown in Figure 8 as a function of the momentum of the neutron. This model shows excellent agreement with the data obtained in E01-015.

3.2 Changes in the experimental setup for the proposed measurement

3.2.1 The ^{4}He target

We plan to use the standard Hall A cryogenic target ladder containing 4 cm and 15 cm cells. Our production target will be ^{4}He gas with LH_2, LD_2, solid carbon optics and aluminum foils for detector and magnet optics calibrations.

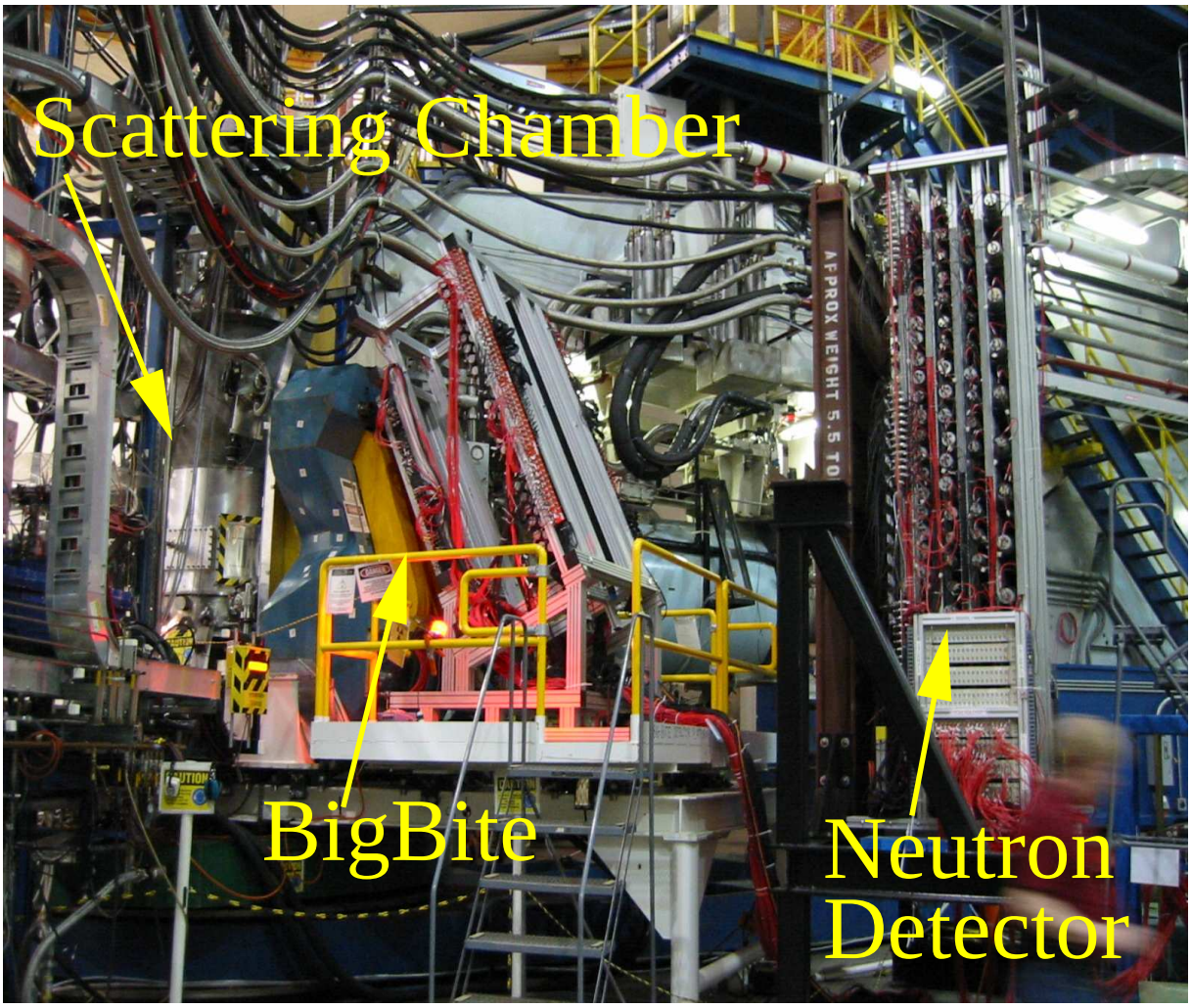

Fig. 7. The BigBite spectrometer system, the neutron array with the lead wall, and the large aperture scattering chamber to match their acceptance are shown in this photo. BigBite consisted of a one Tesla dipole, and two scintillator packages labeled the auxiliary plane and the trigger plane. The neutron array had one veto layer and four scintillator bar layers.

3.2.2 BigBite

The recoiling protons will be detected by the BigBite spectrometer, which will be located 1.1 meters from the target - similar to the setup of E01-015 (see Section 3.1). We plan to use the two back scintillator planes, ΔE and E, for particle identification and TOF, as used in E01-015. However, we plan to replace the auxiliary plane by a thin plane of scintillating fibers, each with a cross section of 2x2 mm^2, laid along the transverse direction. The fibers will be bunched in the dispersive direction in groups of 12 into PMTs on both sides of the fibers, but staggered by 6 fibers on either side to facilitate resolution of 6 fibers (12 mm) in the dispersive direction. The overall dimensions of the auxiliary plane will remain 1400x250 mm^2. In comparison to the auxiliary plane used in E01-015, the new auxiliary plane will provide:

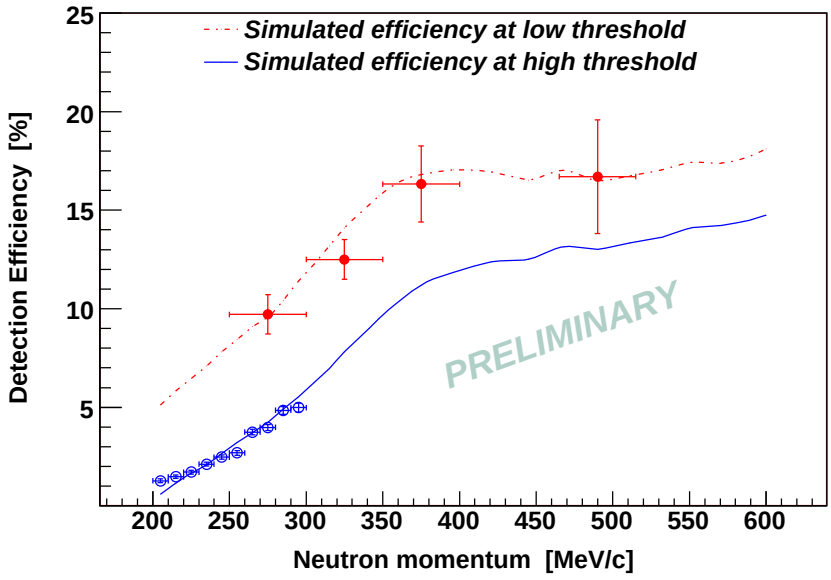

Fig. 8. The simulated and measured neutron detection efficiency in E01-015. In this experimental setup, the lead wall was 5 cm thick and the neutron detector was composed of four scintillator planes.

- A better resolution in the dispersive direction by a factor of 2, resulting in a better momentum resolution.
- A position resolution of about 3 cm in the transverse direction (25 cm in the "old" auxiliary plane). Together with similar information from the ΔE and E planes, this will enable tracing events back to the target which will be very useful in distinguishing "good" from "random" tracks.
- Much better timing information from the 2 PMTs on both sides of the fibers (the "old" auxiliary plane had PMTs only on one side of its scintillators).

3.2.3 The shield wall and the neutron-array

Analysis of the neutron data collected during E01-015 showed that the lead wall thickness was more than adequate for attenuating charged particles and photons originating from the target or showering from material between the target and the neutron detector veto layer. Since the current lead wall attenuated the neutron flux by roughly 50%, we plan to decrease the lead wall thickness to 2.5 cm, reducing the attenuation to about 25%. Simulations of this thinner wall indicate that we will still have adequate attenuation of the photon flux from the target and reasonable singles rates in the scintillator bars. We also plan to modify the existing neutron detector support structure to add two additional layers of 10 cm thick by 1 m long by 25 cm high scintillator bars. These scintillator bars will be provided by Kent State University. These modifications to the neutron detector array and lead wall will increase the overall efficiency for neutron detection from a typical value of 17% (Figure 8) for the neutron momentum range of interest, to roughly 30% (Figure 9).

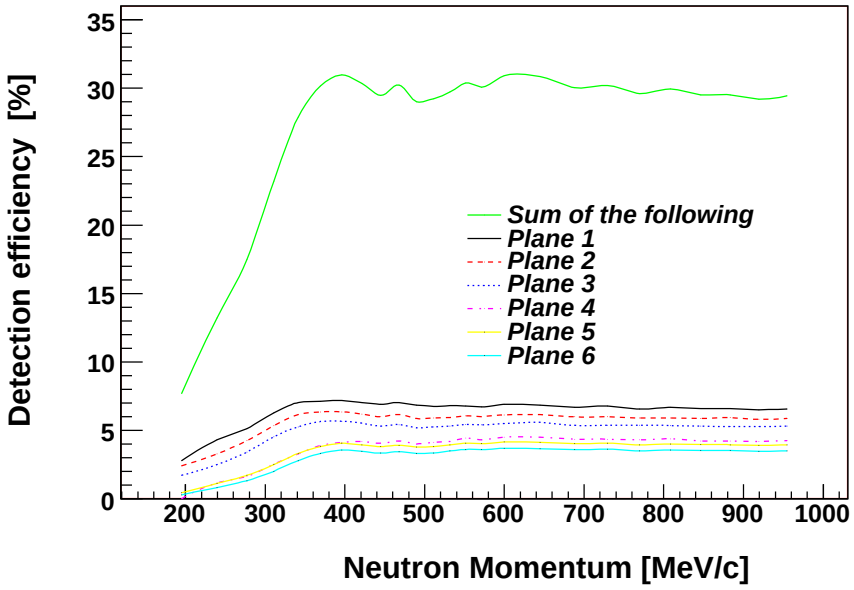

Fig. 9. The simulated neutron detection efficiency for an experimental setup using a lead wall thickness of 2.5 cm and six scintillator planes in the neutron detector.

3.3 Rates

The estimated counting rates for this proposal are based on the E01-015 experiment.

The limiting factor in this triple coincidence experiment with very small cross sections and large solid angle detectors is the nucleon luminosity. In E01-015 we proved that with 30 μA on a 20° tilted 0.25 mm thick ^{12}C foil, we can identify clearly the real triple coincidence signal. The signal to background ratio for the $(e, e'pp)$ and the $(e, e'pn)$ measurements, as measured in E01-015 are shown in Figure 10. We propose to do the measurement at the same nucleon luminosity as E01-015 was done.

In E01-015, for the highest $p_{\rm miss}$ setting of 500 MeV/c, we detected about 100 $(e, e'pp)$ and 100 $(e, e'pn)$ events. This was done with an integrated charge of 15 Coulombs, at a beam current of 30 μA for 140 hours (i.e about 6 days). Therefore, the measured rate for an incident electron beam with $E = 4.627$ GeV and $Q^2 = 2$ (GeV/c)^2 on a ^{12}C target with central missing momentum of 500 MeV/c is:

$$20\ (e, e'pp) \text{ and } 20\ (e, e'pn) \text{ events/day.}$$

This rate is the base for the rate estimate in this proposal. As discussed above we plan to change the lead wall and the neutron array to increase the overall neutron detection efficiency. This experiment will run best at the maximum possible energy (5.1 GeV). The higher the energy, the larger the the cross section. For the rate estimates we will assume

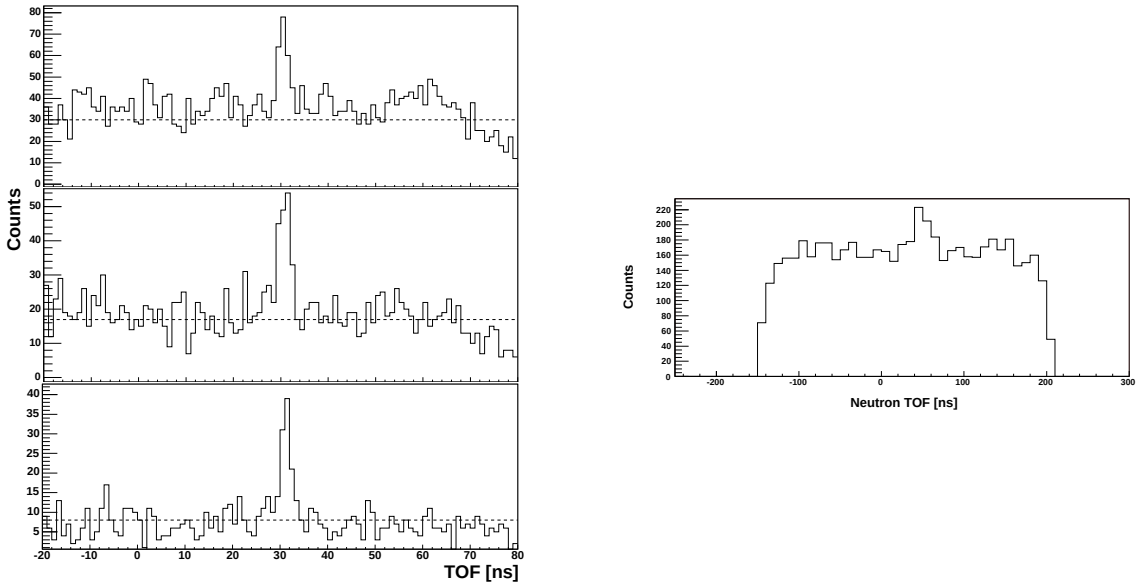

Fig. 10. Left: The measured time of flight (TOF) for protons detected in BigBite in coincidence with electrons and protons in the two HRSs. The TOF was corrected for the trajectory length and the momentum as measured in BigBite without using the TOF information. Right: same for neutrons detected in the neutron array. The peak shown clearly in all spectra is thus due to real triple coincidences and the flat background is due to random coincidences between the ^{12}C$(e,e'p)$ reaction and protons in BigBite (left) or neutrons in the array (right).

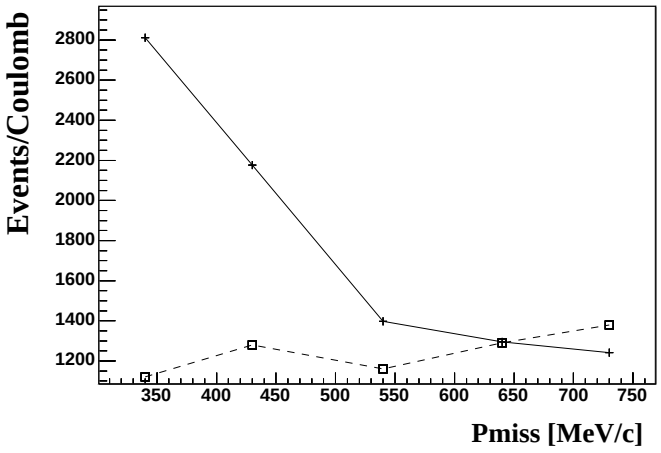

Fig. 11. Solid line: the number of ^{12}C$(e,e'p)$ events per Coulomb of charge as a function of missing momentum as measured in E01-015. Dashed line: the number of ^{12}C$(e,e'p)$ events per Coulomb multiplied by the focusing factor. The dashed line is proportional to the expected triple coincidence rate in this proposal, see text for explanation.

4.8 GeV which will increase the rates, compared to E01-015, by 10%. Therefore, the basic rate for ^{12}C and missing momentum of 500 MeV/c is expected for this proposal to be:

22 $(e,e'pp)$ and 40 $(e,e'pn)$ events/day.

Figure 11 shows the number of $(e, e'p)$ events per Coulomb of beam on target as a function of $p_{\rm miss}$, as was measured in E01-015. We also show the number of events expected per Coulomb, corrected for the focusing effect. The later is due to a smaller angular spread caused by the CM motion of the pair as $p_{\rm miss}$ increases, as well as the finite size of the BigBite/n-array detectors. The focusing factor was estimated using a simulation of scattering off of a moving pair with CM parameter as determined in E01-015 [5,6,23]. As one can deduce from the figure, the expected rate is essentially constant, independent of the missing momentum. To a good approximation the probability for finding a 2N-SRC (as determined from the inclusive (e, e') data [7,8]), the fixed nucleon luminosity, and the nuclear transparency also create a fixed rate independent of the nucleus. We assume that the 2N-SRC fraction of the $(e, e'p)$ is equal at all proposed points. For the count rate estimate, we adjust the $(e, e'pn)$ and $(e, e'pp)$ rates to the expected ratio as shown in Figure 5.

We would like to emphasize the exploratory/speculative nature of the highest missing momentum measurement. At this point the momentum of the recoil and the scattered protons are about equal. Interference terms, as well as non-negligible relativistic effects, might play an important role and may mask the ground state properties of the 2N interaction.

Based on the argument above, the proposed measurement plan, the total number of triple coincidence events and the beam time is summarized in the Table 2.

target	$p_{\rm miss}$ [MeV/c]	days	$(e, e'pp)$ events	$(e, e'pn)$ events
^{4}He	400	5	110	200
^{4}He	500	5	110	200
^{4}He	625	5	235	160
^{4}He	750	5	280	150
^{4}He	875	5	320	140

Table 2
Beam time request and expected triple coincidence rate.

3.4 Requested beam time

- Set up, establishing coincidences, calibrations, background checks: **100 hours**
- Measurements at $Q^2 = 2$ $(GeV/c)^2$. About 1000 (np-SRC) and 1000 (pp-SRC) events in the $p_m = 400 - 875$ MeV/c region. **25 days**
- *TOTAL REQUESTED BEAM HOURS:* **29 days**

3.5 Resources

We summarize here the special resources needed for the experiment. These are in addition to what we already used in the previous E01-015 experiment.

- ^{4}He target, LD2, LH2 - available as a standard Hall A cryogenic targets.
- More neutron counters - These will be acquired from Kent State and JLab (Hall A G_E^n experiment, E02-013). At JLab there are enough power supplies, cables, fast electronics, and readout channels to extend the width of the neutron array to the desired value.
- Frame - We need to design and build a new frame to hold the extra layers of neutron counters.
- A line of sight shield wall. We have to design and build a new lead wall, thiner than the one used for E01-015.
- Readout electronics: We will perform the measurement with the existing readout system that served the E01-015 and the Hall A G_E^n experiment (E02-013). However, we prefer to use flash ADCs so we will not have to decide on thresholds for the neutron detectors but rather determine them using software in the analysis.
- Manpower: The current proposal is essentially the same as E01-015 that was performed successfully in Hall A during 2004/2005. The group proposing this is the E01-015 collaboration which is sufficiently large and experienced to perform the proposed experiment. Graduate students from KSU, TAU, and MIT are expected to take part in this project.

References

[1] Nuclear Science: A Long Range Plan, the DOE/NSF Nuclear Science Advisory Committee, February 1996.

[2] A. D. Shalit and H. Feshbach, *Theoretical Nuclear Physics* (Wiley, New York, 1974).

[3] L. L. Frankfurt and M. I. Strikman, Phys. Rept. **76**, 215 (1981).

[4] L. L. Frankfurt and M. I. Strikman, Phys. Rept. **160**, 235 (1988).

[5] The E01-015 Experiment's Website, http://hallaweb.jlab.org/experiment/E01-015.

[6] E. Piasetzky, W. Bertozzi, J. W. Watson, and S. A. Wood (spokespersons), JLab experiment E01-015, (2001).

[7] K. S. Egiyan *et al.*, Phys. Rev. **C68**, 014313 (2003).

[8] K. S. Egiyan *et al.*, Phys. Rev. Lett. **96**, 082501 (2006).

[9] L. L. Frankfurt, M. I. Strikman, D. B. Day, and M. Sargsian, Phys. Rev. **C48**, 2451 (1993).

[10] J. L. S. Aclander *et al.*, Phys. Lett. **B453**, 211 (1999).

[11] A. Tang *et al.*, Phys. Rev. Lett. **90**, 042301 (2003).

[12] A. Malki *et al.*, Phys. Rev. **C65**, 015207 (2002).

[13] E. Piasetzky *et al.*, Phys. Rev. Lett. **97**, 162504 (2006).

[14] I. Yaron *et al.*, Phys. Rev. **C66**, 024601 (2002).

[15] E. J. Moniz *et al.*, Phys. Rev. Lett. **26**, 445 (1971).

[16] M. M. Sargsian, T. V. Abrahamyan, M. I. Strikman, and L. L. Frankfurt, Phys. Rev. **C71**, 044615 (2005).

[17] R. Schiavilla, R. B. Wiringa, S. C. Pieper, and J. Carlson, nucl-th/0611037 (2006).

[18] SRC 2006 Workshop, http://conferences.jlab.org/SRC2006/index.html.

[19] R. Schiavilla, private communication.

[20] R. Roth, T. Neff, H. Hergert, and H. Feldmeier, Nucl. Phys. **A745**, 3 (2004).

[21] M. Alvioli, C. Ciofi degli Atti, and H. Morita, Phys. Rev. **C72**, 054310 (2005).

[22] M. M. Sargsian and M. I. Strikman, private communication.

[23] R. Shneor *et al.*, to be submitted to Phys. Rev. Lett.

[24] R. G. Arnold *et al.*, Phys. Rev. **C42**, 1 (1990).

[25] J. M. Laget, Phys. Lett. **B199**, 493 (1987).

[26] L. L. Frankfurt, M. M. Sargsian, and M. I. Strikman, Phys. Rev. **C56**, 1124 (1997).

[27] V. R. Pandharipande and S. C. Pieper, Phys. Rev. C **45**, 791 (1992).

[28] I. Mardor *et al.*, Phys. Rev. **C46**, 761 (1992).

[29] J. Alcorn *et al.*, Nucl. Instrum. Meth. **A522**, 294 (2004).

[30] D. W. Higinbotham *et al.*, Nucl. Instrum. Meth., to be submitted.

[31] V. McLane *et al.*, *Neutron Cross Section, Curves, Volume 2* (Academic Press, Boston, 1988).

[32] R. A. Cecil *et al.*, Nucl. Instrum. Meth. **161**, 439 (1979).